21
A relativistic model of the nucleus

In current and future electron scattering studies of nuclei, one is interested in momentum transfers $q^2 \gg m^2$. For consistency, a relativistic description of the nuclear many-body system is required. One such model, *quantum hadrodynamics* (QHD) is developed in detail in [Se86, Se92, Wa95, Se97]. Relativistic mean field theory (RMFT) then includes the strong nuclear interactions in an average fashion. In its simplest version, one starts from a baryon field $\psi = \begin{pmatrix} \psi_p \\ \psi_n \end{pmatrix}$, neutral vector and scalar fields (V_μ, ϕ), and the lagrangian density

$$\begin{aligned}\mathscr{L} &= -\bar{\psi}\left[\gamma_\mu\left(\frac{\partial}{\partial x_\mu} - ig_v V_\mu\right) + (m - g_s\phi)\right]\psi - \frac{1}{2}\left[\left(\frac{\partial\phi}{\partial x_\mu}\right)^2 + m_s^2\phi^2\right] \\ &\quad -\frac{1}{4}F_{\mu\nu}F_{\mu\nu} - \frac{1}{2}m_v^2 V_\mu^2 \end{aligned} \tag{21.1}$$

Here

$$F_{\mu\nu} = \frac{\partial V_\nu}{\partial x_\mu} - \frac{\partial V_\mu}{\partial x_\nu} \tag{21.2}$$

The equations of motion for a field theory are those of continuum mechanics [Bj65a, Fe80, Wa91].

$$\frac{\partial}{\partial x_\mu}\frac{\partial \mathscr{L}}{\partial(\partial q/\partial x_\mu)} - \frac{\partial \mathscr{L}}{\partial q} = 0 \tag{21.3}$$

The Euler–Lagrange equations for the above fields are

$$\left[\left(\frac{\partial}{\partial x_\mu}\right)^2 - m_s^2\right]\phi = -g_s\bar{\psi}\psi$$

https://doi.org/10.1017/9781009290616.026 Published online by Cambridge University Press

$$
\begin{aligned}
\frac{\partial}{\partial x_\nu}F_{\mu\nu} + m_v^2 V_\mu &= ig_v\bar{\psi}\gamma_\mu\psi \\
\left[\gamma_\mu\left(\frac{\partial}{\partial x_\mu} - ig_v V_\mu\right) + (m - g_s\phi)\right]\psi &= 0
\end{aligned} \tag{21.4}
$$

The scalar field couples to the baryon scalar density, the vector field couples to the conserved baryon current, and the Dirac equation for the baryon field has the meson fields included in a minimal, linear fashion. One now imposes canonical (anti-)quantization on the dynamical variables, the fields, and this leads to a *relativistic quantum field theory* [Bj65a, Wa91].

Consider uniform nuclear matter. One can obtain an approximate solution to the field equations by replacing the meson fields by their expectation values, which are then just classical fields. By translation invariance, these quantities must be constants independent of space and time.

$$
\begin{aligned}
\phi \to \langle\phi\rangle &\equiv \phi_0 \\
V_\lambda \to \langle V_\lambda\rangle &= i\delta_{\lambda 4}V_0
\end{aligned} \tag{21.5}
$$

The last equality follows from the isotropy of the medium. This RMFT should become better and better as the baryon density ρ_B gets larger and the sources on the right side of the meson field equations correspondingly increase. At observed nuclear density, this is equivalent to the usual (relativistic) Hartree approximation. With this approximation, the baryon field equation is linearized.

$$
\left[\gamma_\mu\frac{\partial}{\partial x_\mu} + g_v\gamma_4 V_0 + (m - g_s\phi_0)\right]\psi = 0 \tag{21.6}
$$

This linear equation can be solved exactly. Stationary state solutions to the Dirac equation lead to the eigenvalue equation

$$
\begin{aligned}
\varepsilon_k^{(\pm)} &= g_v V_0 \pm \sqrt{\mathbf{k}^2 + m^{\star 2}} \\
m^\star &\equiv m - g_s\phi_0
\end{aligned} \tag{21.7}
$$

The ground state of the corresponding hamiltonian of this RMFT is obtained by filling the Dirac levels up to the Fermi momentum k_F. To be self-consistent, one determines the sources in the meson field equations by summing over the occupied levels

$$
\begin{aligned}
\rho_S &= \langle\bar{\psi}\psi\rangle = \frac{1}{\Omega}\sum_{\mathbf{k}\lambda}^{k_F}\bar{U}(\mathbf{k}\lambda)U(\mathbf{k}\lambda) \\
\rho_B &= \langle\psi^\dagger\psi\rangle = \frac{1}{\Omega}\sum_{\mathbf{k}\lambda}^{k_F}U^\dagger(\mathbf{k}\lambda)U(\mathbf{k}\lambda)
\end{aligned} \tag{21.8}
$$

https://doi.org/10.1017/9781009290616.026 Published online by Cambridge University Press

We choose to normalize to unit probability in the box, so that $U^\dagger U = 1$. Note also the important relation, derived immediately from the Dirac equation

$$\bar{U}(\mathbf{k}\lambda)U(\mathbf{k}\lambda) = \frac{m^\star}{\sqrt{\mathbf{k}^2 + m^{\star 2}}} U^\dagger(\mathbf{k}\lambda)U(\mathbf{k}\lambda) \tag{21.9}$$

From the field equations, for constant fields

$$\phi_0 = \frac{1}{m_s^2}\rho_S \qquad ; \; V_0 = \frac{1}{m_v^2}\rho_B \tag{21.10}$$

The translational invariance of nuclear matter permits ready solution of the resulting coupled, non-linear, differential equations. The quantity $m^\star$ is calculated self-consistently. Nuclear matter saturates at the right binding energy and density in RMFT if one takes

$$C_s^2 \equiv g_s^2 \left(\frac{m^2}{m_s^2}\right) = 267.1 \qquad ; \; C_v^2 \equiv g_v^2 \left(\frac{m^2}{m_v^2}\right) = 195.9 \tag{21.11}$$

The saturation and $m^\star$ curves are shown in [Wa95].

The baryon field operator in RMFT takes the following form

$$\psi(x) = \frac{1}{\sqrt{\Omega}} \sum_{\mathbf{k}\lambda} \left[A_{\mathbf{k}\lambda} U(\mathbf{k}\lambda) \exp{(ik \cdot x)} + B_{\mathbf{k}\lambda}^\dagger V(-\mathbf{k}\lambda) \exp{(-ik \cdot x)} \right] \tag{21.12}$$

Here $A_{\mathbf{k}\lambda}$ destroys a baryon of momentum and helicity $(\mathbf{k}, \lambda)$ in the medium and $B_{\mathbf{k}\lambda}^\dagger$ creates an antibaryon [Bj65a, Fe71, Wa91].

An *effective electromagnetic current operator* is now introduced. The internal structure of the individual nucleons, which from this hadronic point of view arises from charged meson fields, is summarized in a single-nucleon form factor and an effective Mø ller potential

$$\frac{1}{q^2} \rightarrow \frac{f_{\rm SN}(q^2)}{q^2} \tag{21.13}$$

The effective current, to be used in lowest order in the nuclear many-body problem, is then taken to be

$$\begin{aligned} J_\mu(x) &= i\bar{\psi}\gamma_\mu \underline{Q}\psi + \frac{1}{2m}\frac{\partial}{\partial x_\nu}\bar{\psi}\sigma_{\mu\nu}\underline{\lambda}'\psi \\ \underline{Q} &= \frac{1}{2}(1+\tau_3) \\ \underline{\lambda}' &= \lambda_p'\frac{1}{2}(1+\tau_3) + \lambda_n\frac{1}{2}(1-\tau_3) \end{aligned} \tag{21.14}$$

https://doi.org/10.1017/9781009290616.026 Published online by Cambridge University Press

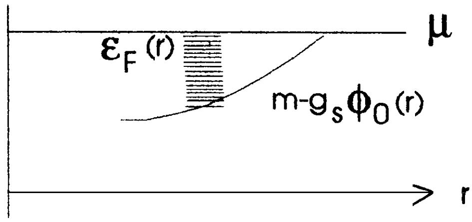

Fig. 21.1. Thomas–Fermi theory for finite systems.

If $\psi(x)$ satisfies the field Eq. (21.6), and its adjoint, then this current is both *local and conserved*

$$\frac{\partial J_\mu(x)}{\partial x_\mu} = 0 \tag{21.15}$$

Furthermore, it gives the correct result for a free nucleon.[1]

An immediate extension of RMFT to finite nuclei is through Thomas–Fermi theory [Se86]. Here one gives the meson fields a spatial variation

$$\begin{aligned}(\nabla^2 - m_s^2)\phi_0(r) &= -\rho_S(r) \\ (\nabla^2 - m_v^2)V_0(r) &= -\rho_B(r)\end{aligned} \tag{21.16}$$

It is then assumed that these fields vary slowly enough so that one can calculate the sources for a uniform system at the appropriate baryon density $\rho_B(r)$ parameterized by $k_F(r)$ as illustrated in Fig. 21.1.[2] The condition $k_F = 0$ determines the nuclear size and baryon number B. The electron scattering cross sections of Rosenfelder for two nuclei $^{40}_{20}\mathrm{Ca(e,e')}$ and $^{208}_{82}\mathrm{Pb(e,e')}$, calculated with local RMFT and then integrated over the Thomas–Fermi distributions, are shown in Figs. 21.2 and 21.3 [Ro80]. The calculations are compared with quasielastic electron scattering data from HEPL on these nuclei [Mo71]. Note the following features of

[1] This effective electromagnetic current assumes $F_1(q^2)/F_1(0) \approx F_2(q^2)/F_2(0) \approx f_{\mathrm{SN}}(q^2)$. This relation breaks down at large q^2 where the data indicate that it is the Sachs form factors $G_M = F_1 + 2mF_2$ and $G_E = F_1 - q^2F_2/2m$ that scale. To incorporate this observation, make the following replacements:

$$\frac{f_{\mathrm{SN}}(q^2)}{q^2} \to \frac{f_{\mathrm{SN}}(q^2)}{q^2}\frac{1}{1+q^2/4m^2}$$
$$J_\lambda \to J_\lambda - \frac{i}{4m^2}\frac{\partial}{\partial x_\nu}\frac{\partial}{\partial x_\nu}\left(\bar{\psi}\underline{\mu}\gamma_\lambda\psi\right)$$

Here $\underline{\mu}$ is the full magnetic moment [Wa95]. Applications of this improved effective current do not exist at the present time.

[2] $k_F^n(r)$ and $k_F^p(r)$ will differ if $N \neq Z$ and the Coulomb interaction is included.

https://doi.org/10.1017/9781009290616.026 Published online by Cambridge University Press

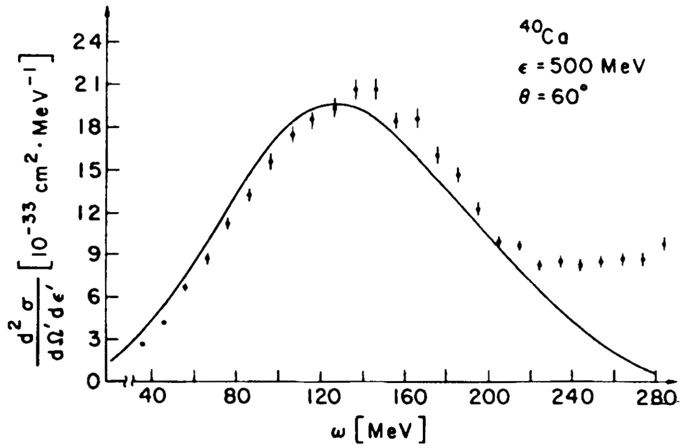

Fig. 21.2. Quasielastic electron scattering from $^{40}_{20}$Ca in RMFT compared with experimental values. The calculation assumes a local Fermi gas with the quantities $m^{\star}(r)$ and $\rho_B(r)$ taken from a relativistic Thomas–Fermi calculation of these quantities in QHD-I [Ro80, Wa95]. Data are from [Mo71].

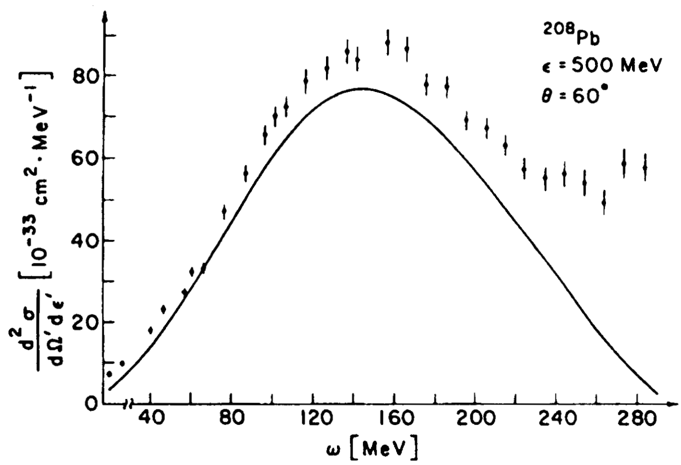

Fig. 21.3. As Fig. 21.2, but for $^{208}_{82}$Pb.

these results:

- They are calculated using the Thomas–Fermi ground state densities;
- The only parameters are those of nuclear matter and $m_s = 550\,\text{MeV}$ from a fit to the mean-square charge radius of $^{40}_{20}$Ca;
- The final result involves values of $m^{\star}(r)$ and $\rho_B(r)$ taken over the entire nuclear density;

https://doi.org/10.1017/9781009290616.026 Published online by Cambridge University Press

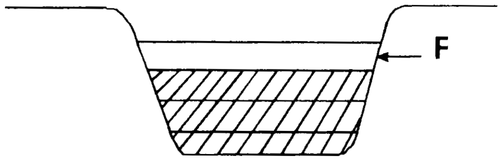

Fig. 21.4. Occupied Dirac orbitals in relativistic Hartree theory.

- It is satisfying that the positions of the peak and values of k_F are approximately correct.[3]

A more satisfactory treatment of finite nuclei is obtained through *relativistic Hartree theory*. Here one solves the Dirac equation in the fields $[\phi_0(r), V_0(r)]$ and assumes the Dirac orbitals are occupied up to some level F in these mean fields as illustrated in Fig. 21.4.[4] The source terms in the meson field equations at a given point are then calculated self-consistently by summing over the contributions of the occupied orbitals

$$\begin{aligned}\rho_B(r) &= \sum_{\alpha}^{F} \phi_{\alpha}^{\dagger}(\mathbf{r})\phi_{\alpha}(\mathbf{r}) \\ \rho_S(r) &= \sum_{\alpha}^{F} \bar{\phi}_{\alpha}(\mathbf{r})\phi_{\alpha}(\mathbf{r})\end{aligned} \tag{21.17}$$

The meson field Eqs. (21.16) are then solved with these sources.

Since the relativistic Hartree calculations provide a very powerful way of dealing with the relativistic nuclear many-body problem, and since they follow from our discussion of the Dirac equation in chapter 10, we digress to develop them [Bj65, Sc68, Se86, Wa95]. Consider the hamiltonian for a Dirac particle moving in spherically symmetric vector and scalar fields.

$$h = -i\vec{\alpha}\cdot\vec{\nabla} + g_v V_0(r) + \beta[M - g_s\phi_0(r)] \tag{21.18}$$

Define the angular momentum by

$$\vec{J} = \vec{L} + \vec{S} = -i\vec{r}\times\vec{\nabla} + \frac{1}{2}\vec{\Sigma} \tag{21.19}$$

The wave function and spin matrix are written in two-by-two form as

$$\psi = \begin{pmatrix} \psi_A \\ \psi_B \end{pmatrix} \qquad \vec{\Sigma} = \begin{pmatrix} \vec{\sigma} & 0 \\ 0 & \vec{\sigma} \end{pmatrix} \tag{21.20}$$

[3] Note there is no additional average binding energy $\bar{\varepsilon}$ required in these calculations.
[4] We here assume closed shells and spherical symmetry.

https://doi.org/10.1017/9781009290616.026 Published online by Cambridge University Press

One first establishes the following commutation relations (this takes a little algebra)

$$[h, J_i] = [h, \vec{J}^{\,2}] = [h, \vec{S}^{\,2}] = 0 \qquad (21.21)$$

Note $[h, \vec{L}^{\,2}] \neq 0$. Now introduce

$$\begin{aligned} K &\equiv \beta(\vec{\Sigma}\cdot\vec{L}+1) = \beta(\vec{\Sigma}\cdot\vec{J}-1/2) \\ [h,K] &= 0 \end{aligned} \qquad (21.22)$$

To establish the vanishing of the second commutator again takes some algebra.

Now label the eigenvalues of K by $K\psi = -\kappa\psi$. The states can be characterized by the eigenvalues $\{j, s = 1/2, -\kappa, m\}$. One then establishes the following relations

$$\begin{aligned} K^2 &= \vec{L}^{\,2} + \vec{\Sigma}\cdot\vec{L} + 1 = \vec{J}^{\,2} + 1/4 \\ \kappa &= \pm(j+1/2) \end{aligned} \qquad (21.23)$$

It follows from these relations that

$$\begin{aligned} -\kappa\psi_A &= (\vec{\sigma}\cdot\vec{L}+1)\psi_A \\ -\kappa\psi_B &= -(\vec{\sigma}\cdot\vec{L}+1)\psi_B \end{aligned} \qquad (21.24)$$

Hence

$$\begin{aligned} \vec{L}^{\,2}\psi_A &= \left[\left(j+\frac{1}{2}\right)^2 + \kappa\right]\psi_A = l_A(l_A+1)\psi_A \\ \vec{L}^{\,2}\psi_B &= \left[\left(j+\frac{1}{2}\right)^2 - \kappa\right]\psi_B = l_B(l_B+1)\psi_B \end{aligned} \qquad (21.25)$$

Thus, although ψ is not an eigenstate of $\vec{L}^{\,2}$, the upper and lower components are separately eigenstates with eigenvalues determined from these relations. They also have fixed j and $s = 1/2$.

Now introduce spin spherical harmonics

$$\Phi_{\kappa m} = \sum_{m_l m_s} \langle l m_l \tfrac{1}{2} m_s | l \tfrac{1}{2} j m\rangle Y_{l m_l}(\theta,\phi)\chi_{m_s} \qquad (21.26)$$

Here $j = |\kappa| - 1/2$. Hence one shows that the solutions to this Dirac equation take the form

$$\psi_{n\kappa m} = \frac{1}{r}\begin{pmatrix} iG(r)_{n\kappa}\Phi_{\kappa m} \\ -F(r)_{n\kappa}\Phi_{-\kappa m} \end{pmatrix} \qquad (21.27)$$

Here $l = \kappa$ if $\kappa > 0$ and $l = -(\kappa+1)$ if $\kappa < 0$.

https://doi.org/10.1017/9781009290616.026 Published online by Cambridge University Press

Consider the relativistic Hartree equations.

$$\begin{aligned}
(\nabla^2 - m_s^2)\phi_0 &= -g_s\rho_S(r) \\
(\nabla^2 - m_v^2)V_0 &= -g_v\rho_B(r) \\
\left(\frac{1}{i}\boldsymbol{\alpha}\cdot\nabla + g_v V_0(r) + \beta[M - g_s\phi_0(r)]\right)\psi &= i\frac{\partial\psi}{\partial t}
\end{aligned} \tag{21.28}$$

Label the baryon states by $\{\alpha\} = \{n\kappa t, m_\alpha\} \equiv \{a, m_\alpha\}$. Here $t = 1/2\,(-1/2)$ for protons (neutrons). Look for stationary state solutions, and insert the form of Dirac wave functions in Eq. (21.27). One needs the following identity, again established with a little work

$$\vec{\sigma}\cdot\vec{\nabla}\,\frac{1}{r}G\Phi_{\kappa m} = -\frac{1}{r}\left(\frac{d}{dr} + \frac{\kappa}{r}\right)G\Phi_{-\kappa m} \tag{21.29}$$

The required relation for F is obtained with the substitution $\kappa \to -\kappa$. It then follows that the coupled radial Dirac equations reduce to

$$\begin{aligned}
&\frac{d}{dr}G_a(r) + \frac{\kappa}{r}G_a(r) - [E_a - g_v V_0(r) + M - g_s\phi_0(r)]F_a(r) = 0 \\
&\frac{d}{dr}F_a(r) - \frac{\kappa}{r}F_a(r) + [E_a - g_v V_0(r) - M + g_s\phi_0(r)]G_a(r) = 0
\end{aligned} \tag{21.30}$$

The normalization condition on the Dirac wavefunctions reduces to

$$\int_0^\infty dr(|G_a(r)|^2 + |F_a(r)|^2) = 1 \tag{21.31}$$

Consider the relativistic Hartree Eqs. (21.28) for the meson fields. For the source terms one uses the following relation for the Dirac solutions if $\kappa = \pm\kappa'$.

$$\sum_{m=-j}^{m=j}\Phi^\dagger_{\kappa m}\Phi_{\kappa' m} = \delta_{\kappa\kappa'}\,\frac{2j+1}{4\pi} \qquad ; \ \kappa = \pm\kappa' \tag{21.32}$$

Hence the meson field equations become

$$\begin{aligned}
\frac{d^2}{dr^2}\phi_0(r) + \frac{2}{r}\frac{d}{dr}\phi_0(r) - m_s^2\phi_0(r) &= -g_s\sum_a^{\rm occ}\left(\frac{2j_a+1}{4\pi r^2}\right)[|G_a(r)|^2 - |F_a(r)|^2] \\
\frac{d^2}{dr^2}V_0(r) + \frac{2}{r}\frac{d}{dr}V_0(r) - m_v^2 V_0(r) &= -g_v\sum_a^{\rm occ}\left(\frac{2j_a+1}{4\pi r^2}\right)[|G_a(r)|^2 + |F_a(r)|^2]
\end{aligned} \tag{21.33}$$

In practice, these relativistic Hartree equations are enlarged to include a condensed neutral ρ field $b_0(r)$ coupled to the third component of the

https://doi.org/10.1017/9781009290616.026 Published online by Cambridge University Press

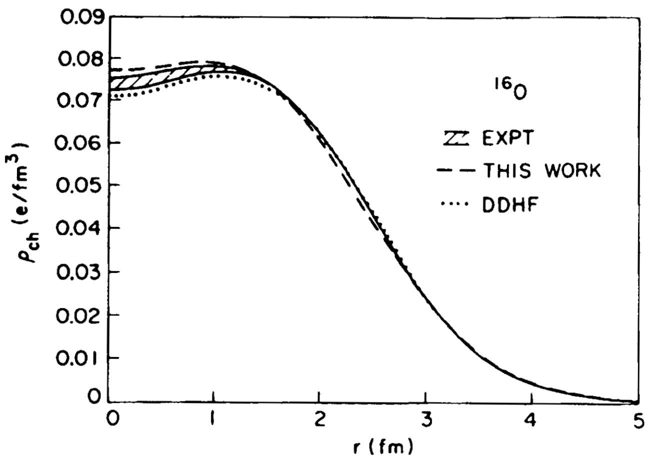

Fig. 21.5. Predicted charge density for $^{16}_{8}$O in the relativistic Hartree model [Ho81, Se86]. The solid curve and shaded area represent the fit to experimental data [Mc69]. Theoretical results are indicated by the long dashed lines [Ho81, Wa95].

isovector baryon density $g_\rho \psi^\dagger \frac{1}{2}\tau_3 \psi$ and the Coulomb field $A_0(r)$ coupled to the charge density $e_p \psi^\dagger \frac{1}{2}(1+\tau_3)\psi$. The extension of the above equations is immediate.

The resulting relativistic Hartree equations are coupled, non-linear differential equations; however, they are *local*. Fortunately, a rapidly convergent computer program has been published, available to all, that solves these equations by iteration [Ho91].

Let us return to applications of this relativistic Hartree theory. Horowitz and Serot [Ho81] make the model more realistic by adding the condensed, neutral ρ field and the Coulomb interaction. The four parameters in their theory (g_v, g_s, g_ρ, m_s) are fitted to the bulk properties of nuclear matter $(E/B, k_F, a_4)_{nm}$ and the root-mean square charge radius of $^{40}_{20}$Ca. Their results are discussed in detail in [Wa95]; the principal features are:

- One finds an excellent fit to ground-state charge densities throughout the periodic table;
- There is a strong spin–orbit interaction, and one derives the single-particle spectrum of the nuclear shell model;
- If one forms a Dirac optical potential from the relativistic Hartree densities and the empirical, Lorentz covariant N–N scattering amplitude (RIA), one obtains a quantitative description of p–A scattering, including the spin observables, up to ≈ 1 GeV.

https://doi.org/10.1017/9781009290616.026 Published online by Cambridge University Press

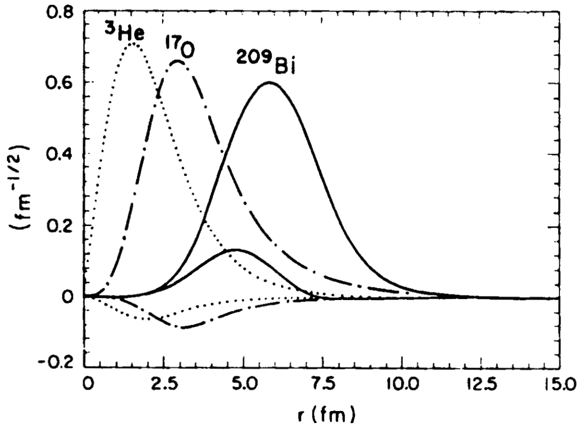

Fig. 21.6. Upper and lower component Dirac radial wave functions $G(r)$ and $F(r)$ for the three cases discussed in the text [Ki86, Wa95].

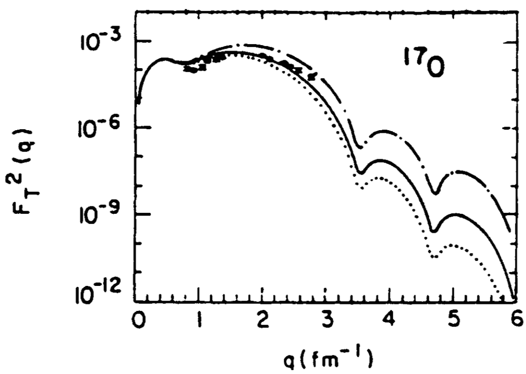

Fig. 21.7. Magnetic form factor squared for $^{17}_{8}$O. Calculated using relativistic Hartree wave functions and the effective current operator [Ki86, Wa95]. The dotted curve omits the C-M correction factor taken from the harmonic oscillator shell model, and the dashed curve omits the single-nucleon form factor. Data are from [Co65, Mc77, Ar78, Ca82].

As a first application of this relativistic Hartree model to electron scattering, consider elastic electron scattering from the extended charge distribution in oxygen $^{16}_{8}$O(e, e). The central density in $^{208}_{82}$Pb determines $(k_F)_{nm}$. The mean-square radius of $^{40}_{20}$Ca determines the one length parameter in the model. The charge distribution of $^{16}_{8}$O is then predicted [Ho81]. It is compared with the experimental determination of this charge distribution in Fig. 21.5. The agreement is all that one might hope for.

As a second application to electron scattering, consider elastic magnetic scattering from $^{17}_{8}$O(e, e). Figure 21.6 shows the Dirac radial wave functions for the valence nucleon, calculated in relativistic Hartree, for three nuclei: $^{3}_{2}\text{He}(\nu 1s)^{-1}_{1/2}$; $^{17}_{8}\text{O}(\nu 1d)_{5/2}$; $^{209}_{83}\text{Bi}(\pi 1h)_{11/2}$ [Ki86, Wa95]. The transverse

https://doi.org/10.1017/9781009290616.026 Published online by Cambridge University Press

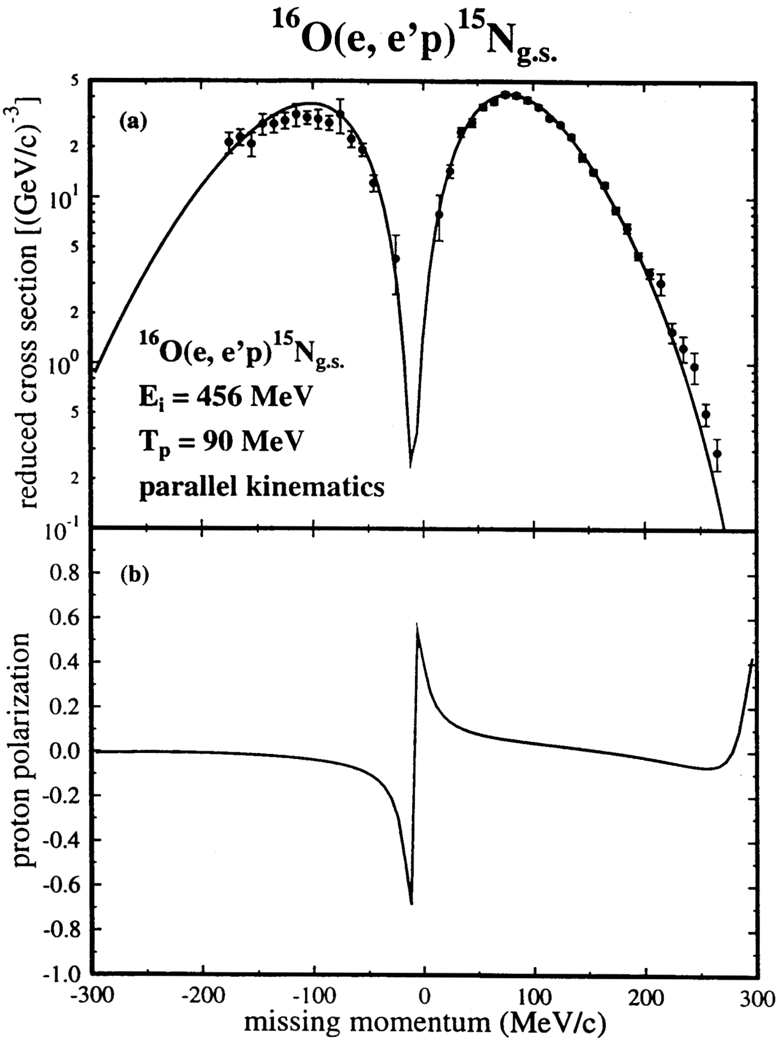

Fig. 21.8. Relativistic Hartree calculation using RIA optical potential and effective current compared with data for ${}^{16}_{8}\mathrm{O}(\mathrm{e},\mathrm{e}'\mathrm{p})^{15}_{7}\mathrm{N}_{\mathrm{g.s.}}$ (see text) [He95]. The author is grateful to J. I. Johansson for preparing this figure.

magnetic form factor for elastic electron scattering from ${}^{17}_{8}\mathrm{O}(\nu 1d)_{5/2}$ calculated by Kim is shown in Fig. 21.7, together with the existing experimental data [Ki86]. Here we again use for the inclusive process

$$\begin{aligned} \frac{d\sigma}{d\Omega} &= 4\pi\sigma_M F^2 r \\ F^2 &\equiv \left(\frac{q_\mu^4}{\mathbf{q}^4}\right) F_L^2 + \left(\frac{q_\mu^2}{2\mathbf{q}^2} + \tan^2\frac{\theta}{2}\right) F_T^2 \end{aligned} \tag{21.34}$$

https://doi.org/10.1017/9781009290616.026 Published online by Cambridge University Press

All the parameters in the calculation are determined through relativistic Hartree and the effective current. The agreement with experiment is satisfactory (but note the scale!), and there is nothing intrinsic in the model that now limits the range of q^2 to which the calculation can apply.[5]

As a third application, consider the electron scattering coincidence reaction ${}^{16}_{8}\mathrm{O}(\mathrm{e}, \mathrm{e}'\,\mathrm{p}){}^{15}_{7}\mathrm{N}_{\mathrm{g.s.}}$. Figure 21.8 shows a state-of-the-art calculation of the cross section for this $(\mathrm{e}, \mathrm{e}'\,\mathrm{p})$ reaction on ${}^{16}_{8}\mathrm{O}$ leading to the $(\pi 1p)^{-1}_{1/2}$ ground state of ${}^{15}_{7}\mathrm{N}$. The calculation is from [He95] and the data from [La93, Le94]. The calculation has the following features:

- Relativistic Hartree wave functions [Ho81] and the Dirac RIA optical potential [Co93] are used, along with the effective electromagnetic current;[6]
- Parallel kinematics $\mathbf{q} \| \mathbf{k}$ are assumed. The missing momentum is defined by

$$\mathbf{p}_m \equiv \mathbf{q} - \mathbf{k} \tag{21.35}$$

  The incident electron energy is 456 MeV and $|\mathbf{q}|$ is held fixed at 90 MeV;
- The ordinate is $d^5/d\varepsilon_2 d\Omega_2 d\Omega_q$ divided by $I_{\mathrm{inc}}\,\sigma_{ep}$ where σ_{ep} is calculated under the same kinematics, but with[7]
  1. An initial proton four-momentum $p_\mu = (\mathbf{p}_m,\ [\mathbf{p}_m^2 + (m - E_S)^2]^{1/2})$, where E_S is the separation energy of the $1p_{1/2}$ proton in ${}^{16}_{8}\mathrm{O}$;
  2. A nucleon vertex $\Gamma_\mu \equiv \gamma_\mu(F_1 + 2mF_2) - (p + q)_\mu F_2$.
- The theoretical calculation has been reduced by a spectroscopic factor of S = 0.69. This represents partial occupancy of the $(1p)_{1/2}$ state in ${}^{16}_{8}\mathrm{O}$ in this model. (See e.g. [Do75].) The shape of the momentum distribution is unaffected by this overall factor;
- The normal polarization of the outgoing proton is also shown. Since the most important consequence of relativistic Hartree theory and RIA is the prediction of the spin–orbit effects, it is crucially important to see how these predictions hold up for nucleons ejected from orbits in the nuclear interior;

[5] Except for a proper relativistic treatment of the C-M motion (see [Ki87]).

[6] To the extent that the relativistic Hartree calculations generate the real part of the empirical RIA optical potentials, this electromagnetic current is conserved. Current conservation in the presence of the imaginary part of the optical potential is a more challenging problem under active investigation.

[7] The denominator is a well-defined expression under all kinematic conditions — it yields the so-called CC1 expression of de Forest [de83].

https://doi.org/10.1017/9781009290616.026 Published online by Cambridge University Press

- There is nothing intrinsic in the calculation that limits the k_μ^2 to which it can be extended, nor the $\mathbf{q}$, provided the RIA optical potential still yields a good description of the scattering.[8]

Quasielastic electron scattering for ${}^{40}_{20}\mathrm{Ca}(\mathrm{e},\mathrm{e}')$ is calculated in relativistic Hartree by summing over single-particle transitions, and including the random phase approximation (RPA) response, in [Ho89].

As described here, QHD is a simple model which reproduces many important aspects of nuclear structure. A much deeper basis for this relativistic quantum field theory approach to the nuclear many-body problem can be given in terms of *effective field theory*. One chooses to use hadronic degrees of freedom as generalized coordinates and writes the most general low-energy lagrangian consistent with the symmetry properties of QCD (chapter 25). This provides the density functional for the nuclear system, and minimization of that density functional leads to the relativistic Hartree equations (with additional non-linear couplings). The values of $g_s\phi_0/m$ and $g_v V_0/m$, both $\approx 1/3$, then yield expansion parameters which provide controlled approximation schemes. This approach puts the RMFT on a much firmer theoretical basis [Fu97, Se97].

[8] Again, except for a proper relativistic treatment of C-M motion.

https://doi.org/10.1017/9781009290616.026 Published online by Cambridge University Press